Eur Biophys J (2001) 30: 250–255
DOI 10.1007/s002490100137

ARTICLE

**Jagannathan Ramesh · Ahmad Salman
Ziad Hammody · Beny Cohen · Jacob Gopas
Nili Grossman · Shaul Mordechai**

FTIR microscopic studies on normal and H-*Ras* oncogene transfected cultured mouse fibroblasts

Received: 7 September 2000 / Revised version: 4 January 2001 / Accepted: 11 January 2001 / Published online: 6 March 2001
© Springer-Verlag 2001

Abstract Infrared absorption spectra are well known for their sensitivity to composition and three-dimensional structure of biomolecules. The biochemical changes in the sub-cellular levels developing in abnormal cells, including a majority of cancer forms, manifest themselves in different optical signatures, which can be detected by IR spectroscopy. We measured the IR absorption spectra of monolayers of cultured normal and H-*ras* transfected mouse fibroblasts, using a microscopic Fourier transform IR (micro-FTIR) technique. The absorption of normal cells was found to be higher than the malignant ones in the spectral range 600–3200 cm^{-1}. The carbohydrate and phosphate contents were higher in normal cells relative to H-*ras* transfected cells. An increase in the RNA/DNA ratio was observed for *H-ras* transfected fibroblasts, which correlates with the increased transcriptional activity expected for the cancerous cells. In part, the variation in absorbance between normal and *ras* transfected fibroblasts may be due to changes in the cell dimensions.

J. Ramesh · A. Salman · Z. Hammody · S. Mordechai (✉)
Department of Physics, Ben-Gurion University,
Beer-Sheva 84105, Israel
E-mail: shaulm@bgumail.bgu.ac.il

B. Cohen
Department of Chemistry, Ben-Gurion University,
Beer-Sheva 84105, Israel

J. Gopas
Department of Microbiology & Immunology,
Faculty of Health Sciences,
Ben-Gurion University and Department of Oncology,
Soroka University Medical Center,
Beer-Sheva 84101, Israel

N. Grossman
Department of Microbiology & Immunology,
Faculty of Health Sciences,
Ben-Gurion University and Skin Bank Laboratory,
Skin Bank and Investigative Dermatology,
Soroka University Medical Center,
Beer-Sheva 84101, Israel

Keywords Cancer · Mouse fibroblasts · *Ras* oncogene · Fourier transform IR microscopy · Spectral fitting

Introduction

Among the spectroscopic techniques available today, Fourier transform infrared (FTIR) microscopy is becoming a powerful tool in the field of biology and medicine. Various molecular components of the cell give a characteristic IR spectrum, which is rich in structural and functional aspects (Jackson et al. 1998; Mantsch and Chapman 1996). One of the most promising applications of the IR-based techniques, which has become possible now, is in biomedicine. IR spectroscopy can detect and monitor characteristic changes in molecular composition and structure that accompany transformation from the normal to the cancerous state (Afanasyeva et al. 1998a; Lasch and Naumann 1998; Mordechai et al. 2000). IR spectroscopy opens new and modern areas of medical research, as it causes no damage to the cells. For the last few years, FTIR microscopic techniques have been used for diagnosis of various types of cancer of human tissues and also for characterization of different kinds of cells (Diem et al. 1999; Franck et al. 1998).

Cancer has been recently recognized as a genetic disease, in which a series of mutations, which can be inherited or acquired, accumulate with time and transform the cells into a malignant phenotype. Causative agents include chemical and environmental carcinogens and tumor promoters, including radiation, transformation by DNA viruses or RNA retroviruses, and genetic inherited predisposition, for example defective DNA repair mechanisms (Cole 1996; Little 2000; Rosenberg and Jolicoeur 1997; Tsao 2000). Normal cells transform into malignancy by activation of oncogenes, derived from mutated growth-controlling genes, encoding growth factors, receptors, intracellular signal transducers, nuclear transcription factors and cell cycle control proteins, and/or inactivation of tumor-suppressor genes.

The *ras* oncogenes, encoding GTP binding proteins with GTPase activity, were originally discovered in murine sarcoma viruses, and were the first nonviral oncogene to be recognized. Over-expression of *ras* and *ras* mutations has been described in various human tumors, such as oral or head and neck squamous cell carcinoma, lung cancer, and in pancreatic carcinoma (Barbacid 1987; Lohr et al. 2000; Scully et al. 2000; Tockman 1996). Reports of *ras* activation and mutations in benign pancreatitis in humans (Lohr et al. 2000) and preceding the onset of neoplasia in an experimental models of carcinogenesis (Kumar et al. 1990) suggest that *ras* may have an early role in neoplasia and emphasize the need for early detection of *ras* harboring cells.

In addition to the numerous biochemical studies of *ras* activation, the reaction mechanisms of *ras* were investigated at the molecular level using biophysical methods, including time-resolved FTIR spectroscopy (Cepus et al, 1998; Gewert 1999). While FTIR microscopy was studied towards differentiation of malignant from healthy cells and tissues, it was not applied for investigating the specific effect of *ras* on the spectral characteristics of malignant cells. Hence, the goal of the present study was to characterize and compare the FTIR microscopic spectra of murine tumorigenic fibroblasts overexpressing H-*ras* relative to their paired cells expressing the normal gene product. Following normalization, the absorption of normal cells was higher than those of malignant cells, suggesting that these cell lines differed in biochemical characteristics, induced specifically by the *ras* oncogene.

Materials and methods

Cell lines

Balb/c 3T3 murine fibroblasts were transfected with H-*ras* oncogene cloned into the selectable plasmid pSV2neo (Tainsky et al. 1987). The resultant clone showed a high tumorigenicity in Balb/c mice and a transformed morphology in vitro. Control cells that were transfected only with the vector plasmid were not tumorigenic and showed normal morphology in vitro (Ehrlich et al. 1994; Gopas et al. 1992). Cells were grown in DMEM supplemented with 10% fetal calf serum, glutamine (2 mM), and antibiotics (penicillin 100 U/mL, streptomycin 100 μg/mL, and gentamycin 50 μg/mL). Growth conditions were 37 °C, 95% humidity, and 8% CO_2. Cells were maintained at pre-confluence and their morphology was routinely inspected. Tissue culture media and materials were purchased from Biological Industries (Beth Haemek, Israel) and tissue culture dishes were from Corning (New York).

Sample preparation

For micro-FTIR measurements, cells were seeded directly on ZnSe (highly transparent to IR) crystals at concentrations of one million cells/slide (6.25 cm^2), while in growth medium lacking phenol red. Twenty fours hours later, excess medium was dried off the slides and data collection was performed.

Data acquisition

FTIR measurements were performed in transmission mode. For the transmission measurement we used an IRscope II with a MCT detector which was coupled to the FTIR spectrometer (Bruker Equinox model 55/S, Opus software). The microscope was also equipped with a CCD camera for the visible range of the spectrum. The measured spectra cover the wavenumber range 600–4000 cm^{-1} in the mid-IR region. During each measurement, the measured sites were about 50×50 μm^2 at most. Such an area contained only a few fibroblasts. The spectrum was taken as an average of 128 scans to increase the signal-to-noise ratio. The baseline was corrected as follows. Initially, the spectrum was divided into 64 sections of equal size. Then the *y*-value minima of the spectrum were connected, giving best fit to the background, and the spectra were normalized arbitrarily to 2 for the amide I peak at 1648 cm^{-1} after baseline correction. For each sample the spectrum was measured at five different microscopic sites of the slide. Measurements were made on a minimum of five pairs of samples and were compared to check for reproducibility.

Spectral analysis and fitting procedures

The band fitting analysis was performed using the software PEAKFIT (version 4.0). The measured spectra were fitted using a standard Gaussian peak shape satisfying the following relationship:

$$I(v) = I_0 \exp\left[-\frac{1}{2}\left(\frac{v - v_0}{w}\right)^2\right] \quad (1)$$

where $I(v)$ represents the IR absorbance at wavenumber v, v_0 is the peak centroid, and w is the width parameter (Afanasyeva et al. 1998b; Lucassen et al. 1998). The full width at half maximum (FWHM) of the band Γ is calculated using the relation:

$$\Gamma = 2.36\, w(\mathrm{cm}^{-1}) \quad (2)$$

A linear function was used to fit residual background. With the enhanced resolution achieved due to the high signal-to-noise ratio, the weak absorption bands can be resolved with high accuracy. Firstly, the second derivative spectrum was generated. The second derivative spectrum was used in identifying the hidden peaks. Secondly, the peaks obtained from the second derivative spectrum were fitted allowing the centroids, widths, and absorption amplitudes to vary simultaneously in the process generating the best spectral fit to the data. The above analysis yielded reliable fits for the entire region of the spectra. The integrated intensities were calculated using Opus software to quantify the metabolites for normal and *ras* transfected samples.

Results

Typical IR absorption spectra of normal fibroblasts in the range 600–4000 cm^{-1} are shown in Fig. 1. The spectrum is dominated by two absorbance bands at 1648 and 1544 cm^{-1}, known as amide I and II, respectively. Amide I arises from the C=O hydrogen bonded stretching vibrations, and amide II from the C-N stretching and a CNH bending vibrations. The weaker protein bands at 1454 and 1401 cm^{-1} are associated with the asymmetric and symmetric CH_3 bending vibrations. The absorption peaks at 1241 and 1086 cm^{-1} are due to the PO_2^- ionized asymmetric and symmetric stretching, respectively. The bands at 3293 and 2924 cm^{-1} are $CH_2$and CH_3 stretching vibrations of cholesterol and phospholipids, respectively. FTIR spectra of normal (two different batches) and H-*ras* transfected fibroblasts (two different batches) are displayed in Fig. 2. The absorption of normal cells was larger than the cancerous types in this entire region (600–3200 cm^{-1}) of the

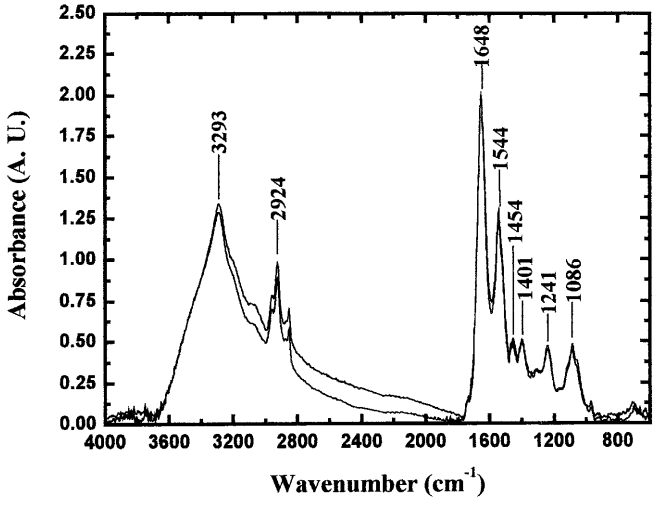

Fig. 1 Infrared microspectroscopy of two samples of normal mouse fibroblasts

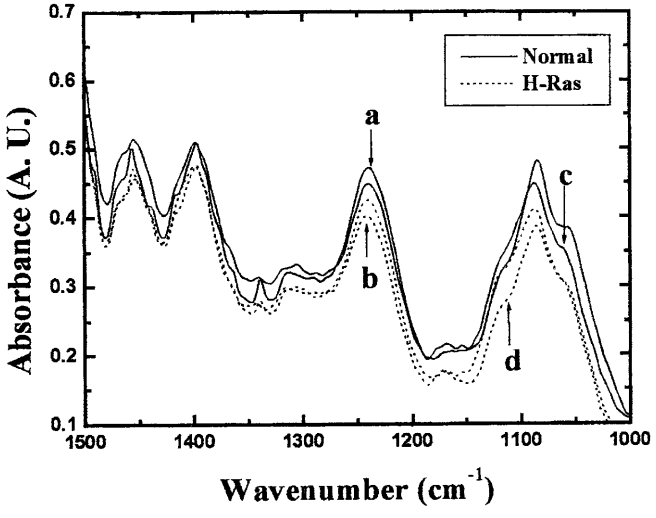

Fig. 2 Infrared microspectroscopy of two normal and H-*ras* transfected mouse fibroblasts. The spectra labeled *a*, *c* and *b*, *d* are normal and H-*ras* transfected fibroblasts of two different batches, respectively

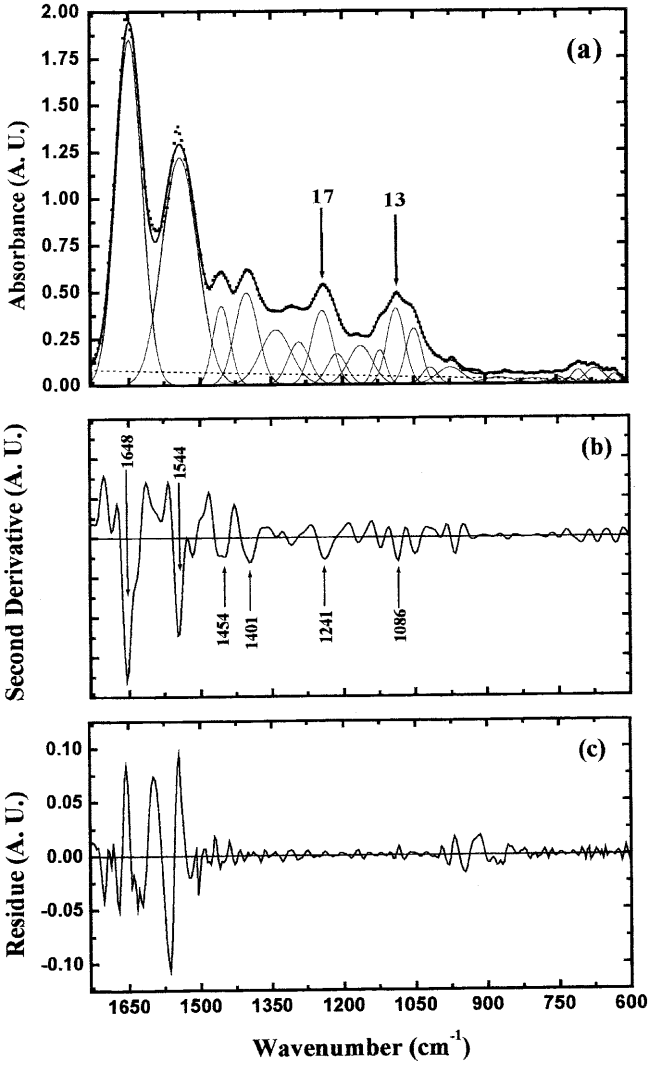

Fig. 3 a Typical band fitting analysis in the wavenumber region 1730–600 cm^{-1} for sample number 5 (normal cells). **b** Second derivative spectrum used for assignments of peak centroids

spectrum in all our samples. Similar notable spectral differences between normal and *ras* transfected types were observed in all the cases studied.

Spectral analysis and band fitting performed for the region 600–1730 cm^{-1} in the present work is shown in Fig. 3a and b. The exact peak location of the bands and "hidden" peaks, which appear on the shoulder of major peaks, were extracted using the second derivative spectra. Figure 3b shows a typical case for normal cells. Figure 3c shows the residue of the above spectral fit. Similar residue spectra (not shown) were obtained for cancerous cells. The same fitting procedure was used for all the normal and malignant fibroblast samples. The analytical area calculated for peaks 13 and 17 (located at 1086 and 1241 cm^{-1}, which arise from the symmetric and asymmetric phosphate stretching vibrations, respectively) for normal and cancerous cells, respectively, is shown in Fig. 4. The results indicate that the bands for phosphate levels were higher in normal cells than the *ras* transfected cells in all five cases.

An increasing absorbance at a 1121/1020 ratio from normal to malignant is evident in literature spectra from several different tissues (Andrus and Strickland 1998). This is an index of the cellular RNA/DNA ratio after subtraction of overlapping absorbancies. To test this hypothesis in the present model, the 1121/1020 ratio was calculated for all the samples. The results (displayed in Fig. 5) show that the RNA/DNA ratio was higher for ras transfected than for normal cells in all the cases we have studied.

Figure 6 displays the upper wavenumber region 2600–3200 cm^{-1} for the two types of cells for two samples. Cholesterol, phospholipids, and creatine are the three essential cellular metabolites that absorb at 2800–3200 cm^{-1}. Here also, the magnitude of normal cells is

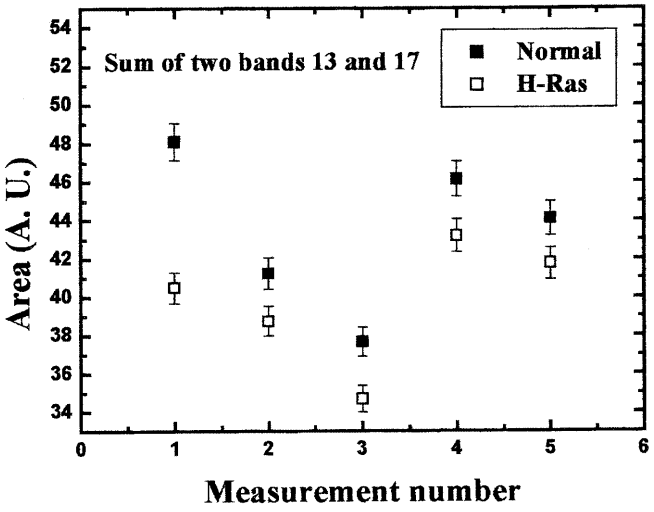

Fig. 4 Summed analytic areas of the two phosphate bands labeled 13 (symmetric) and 17 (asymmetric)

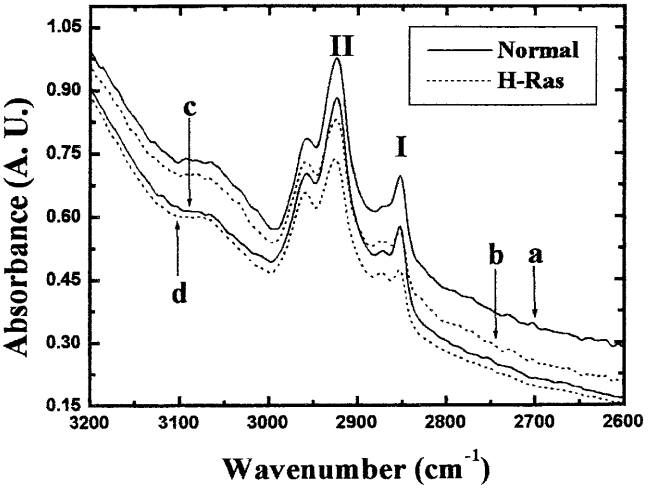

Fig. 6 Infrared microspectroscopy of two normal and H-*ras* transfected mouse fibroblasts in the wavenumber region 2600–3200 cm^{-1}. The spectra labeled *a*, *c* and *b*, *d* are normal and H-*ras* transfected fibroblasts of two different batches, respectively

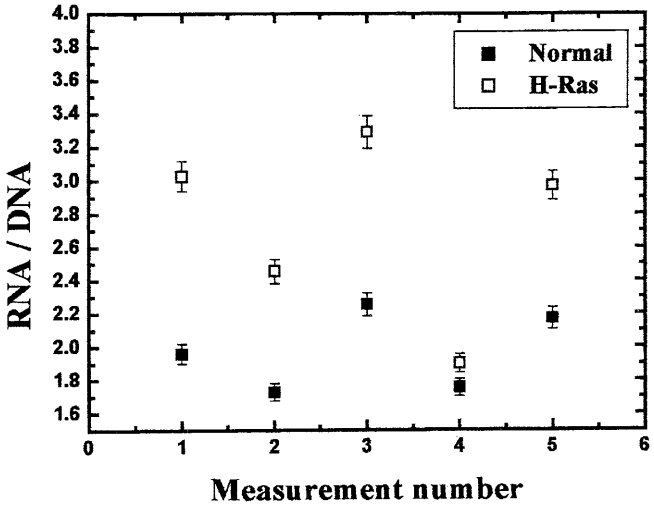

Fig. 5 RNA/DNA ratio for all five normal and H-*ras* transfected fibroblasts calculated from the intensity ratio 1121/1020

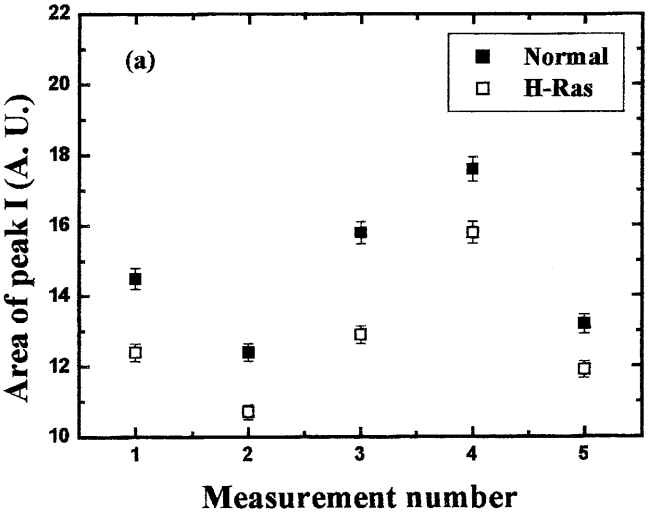

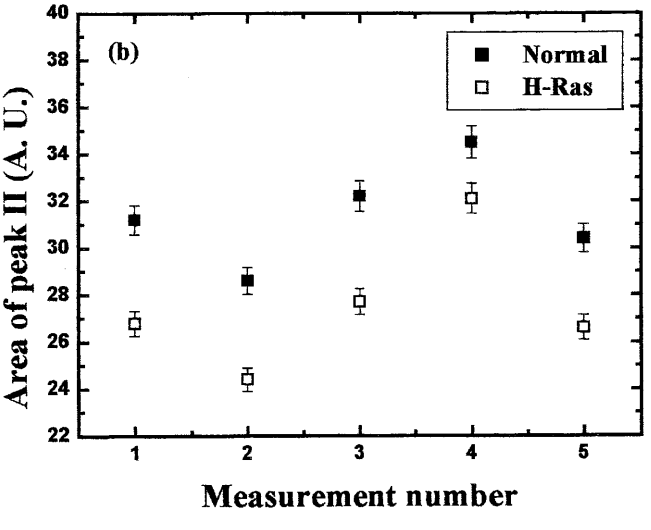

Fig. 7 Integrated area of two peaks: **a** peak I (2866 cm^{-1}) and **b** peak II (2924 cm^{-1}) for five samples

higher than cancerous types in all our samples. Since there are symmetric and asymmetric vibrations due to water in the region 3200–3550 cm^{-1}, this region is not considered for analysis. The integrated intensities for peak I (2866 cm^{-1}) and peak II (2924 cm^{-1}) were calculated by extracting the area under the curve, omitting the baseline underneath using Opus software. The integrated areas calculated for the peaks I and II at 2866 and 2924 cm^{-1} for all five samples are displayed in Fig. 7a and b. The area for normal cells was higher than the cancerous fibroblast cells in all five samples.

The bands at 1025 and 1047 cm^{-1} in the IR spectra are responsible for the vibrational modes of the CH_2OH groups and the C-O stretching coupled with C-O bending of the C-OH groups of carbohydrates (includes glucose, fructose, and glycogen, etc.) (Parker 1971). The ratio of the intensities of the bands at $I(1045)/I(1545)$

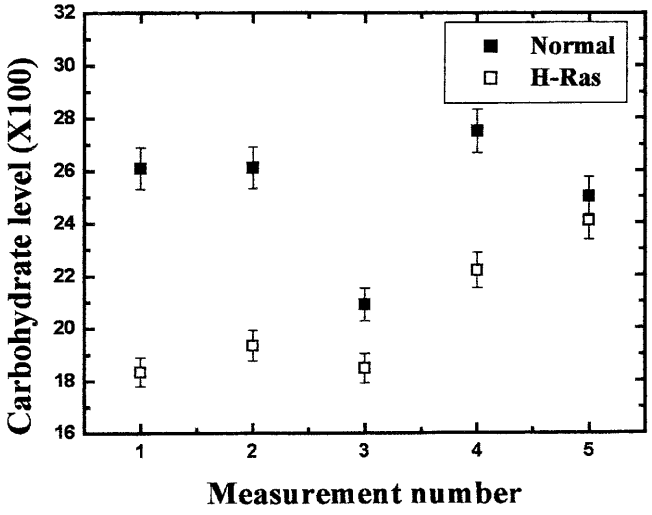

Fig. 8 Carbohydrate levels for all five samples, extracted from the intensity ratio at $I(1045/I(1545)\times100$

gives an estimate of the carbohydrate levels. This analysis is displayed in Fig. 8. Our results indicate that carbohydrate levels were reduced in *ras* transfected cells in comparison with normal cells. This is in complete agreement with the decrease in phosphate levels presented in Fig. 5.

Discussion

The informative PO_2^- symmetrical and asymmetrical stretching vibrations, which occur between 1000 and 1300 cm^{-1}, provide clues to qualitative and quantitative changes for phospholipids and nucleic acids. In our study, the absorption intensity of these vibrations for normal cells was higher than for *ras* transfected types (illustrated by bands 13 and 17 in Figs. 3 and 4). This feature was observed in all cases in the present work. The analysis of phosphate (sym and asym) bands has clearly shown that the total phosphate content is significantly higher in normal cells than the *ras* transfected types.

Our results indicate that the RNA/DNA ratio was increased in the malignant cells relative to normal fibroblasts. These results correlate well with reports available in the literature (Andrus and Strickland 1998). The increased RNA/DNA ratio in the H-ras transfected cells might be explained by their increased metabolic and proliferative activity, relative to the controls. This differential cellular activity is expressed in their different doubling times, determined during the course of the FTIR measurements: 29.0 ± 0.8 h for the *ras* transfected cells and 34.25 ± 1.40 h for the controls. Several reports suggest that the amide I/II intensity ratio increases with DNA content of the cells (Benedetti et al. 1997). We calculated the integrated intensity ratio of amide I/II for all the normal and *ras* transfected fibroblasts (data not shown). The results showed that the DNA content of normal fibroblasts was higher than for the *ras* transfected cells. These results are in good correlation with higher a RNA/DNA ratio for *ras* transfected cells (Fig. 5), which show an increase in RNA and decrease in DNA contents. The same analogy is applicable in the case of normal fibroblasts having a lower RNA/DNA ratio with a higher DNA content. The region between 2800 and 3500 cm^{-1} is due to strong absorption of CH_2 and CH_3 stretching vibrations of phospholipids, cholesterol, and creatine. The integrated areas calculated for the two peaks (at 2866 and 2924 cm^{-1}), labeled peak I and peak II respectively, are shown in Fig. 7a and b. Again, as in the case of the phosphate bands, the intensity for normal cells was higher than for the *ras* transfected type.

Ras genes regulate key cellular signaling pathways (Barbacid 1987). Several lines of evidence indicate that, among other cellular changes, the phospholipid metabolism is altered as a result of oncogene-induced transformation (Tsai et al. 1990). The phospholipid molecules and their metabolites are believed to participate in the processes of oncogene-induced transformation (Lacal and Carnero 1994). Momchilova et al. (1999) reported that all phospholipid fractions were reduced in *ras*-transfected fibroblasts except that for phosphotidylethanolamine (PE). A similar trend was observed in our study also when vector normalization was applied to the spectra (instead of the amide I). This may explain our results that the phosphate content was higher in normal cells than in the *ras* transfected cell lines. The *ras* mediated increase in the transcriptional activity can be the reason for the increase in the RNA/DNA ratio for cancerous cells relative to the normals (Quincoces et al. 1997). The absorption in the range 2800–3000 cm^{-1} is found to be lower for *ras* transformed cells than the normal fibroblasts. The reduction in the levels of phospholipids (CH_2, CH_3 stretching vibrations of phospholipids) in the *ras* transfected cells accounts for our observation. In addition, it is suggested that the higher absorbance over a wide wavelength range (with amide I normalization) of the normal fibroblasts relative to the malignant cells may be attributed in part to the changes in cell dimensions (volume and surface area) of the *ras* transfected fibroblasts, resulting in a relative decrease of subcellular entities.

Summary and conclusions

Our study indicates that FTIR absorption in the range from 600 to 3200 cm^{-1} is lower for tumorigenic *ras* overexpressing mouse fibroblasts than for their paired normal cells. The increased carbohydrate and phosphate contents were observed in normal cells relative to H-*ras* transfected cells. An increase in the RNA/DNA ratio was observed for H-*ras* transfected fibroblasts, which correlates with the increased transcriptional activity expected for the cancerous cells. Our results showed lower cellular contents of phospholipids in the malignant cells,

such as PC, PS, and PA, as reported in the literature. The observed spectral changes may be contributed partly by the changes in the cell dimensions of the *ras* overexpressing cells.

Acknowledgements This research work was supported in part by the Middle East Cancer Consortium (MECC) and the Cancer Research Foundation at the Soroka Medical Center in Memory of Prof. Tabb. Many thanks are due to Dr. V. Erukhimovitch for help with data collection.

References

Afanasyeva NI, Kolyakov FS, Artjushenko SG, Sokolov VV, Frank GA (1998a) Minimally invasive and ex vivo diagnostics of breast cancer tissues by fiber optic evanescent wave Fourier transform IR (FEW-FTIR) spectroscopy. SPIE 3250:140–146

Afanasyeva NI, Kolyakov FS, Leonid NB (1998b) Remote skin tissue diagnostics in vivo by fiber optic evanescent wave Fourier transform infrared (FEW-FTIR) spectroscopy. SPIE 3257:260–266

Andrus PG, Strickland RD (1998) Cancer grading by Fourier transform infrared spectroscopy. Biospectroscopy 4:37–46

Barbacid M (1987) *Ras* genes. Annu Rev Biochem 56:779–827

Benedetti E, Bramanti E, Papineschi F, Rossi I (1997) Determination of the relative amount of nucleic acids and proteins in leukemic and normal lymphocytes by means of FT-IR microspectroscopy. Appl Spectrosc 51:792–797

Cepus V, Scheidig AJ, Goody RS, Gerwert K (1998) Time-resolved FTIR studies if the GTPase reaction of H-*ras* p21 reveal a key role for the beta-phosphate. Biochemistry 37:10263–10271

Cole CN (1996) Polyomavirinae: the viruses and their replication. In: Fields BN, Knipe DM, Howley PM, Chanock RM, Melinick JL, Monath TP, Roizman B, Straus SE (eds) Field's virology, 3rd edn, vol 2. Lippincott-Raven, Philadelphia, pp 1997–2025

Diem M, Boydston-White S, Chiriboga L (1999) Infrared spectroscopy of cells and tissues: shining light onto a novel subject. Appl. Spectrosc 53:148–161

Ehrlich T, Wishniak O, Isakov N, Cohen O, Segal S, Rager-Zisman B, Gopas J (1994) The effect of H-*ras* expression on tumorigenicity and immunogenicity of Balb/c 3T3 fibroblasts. Immunol Lett 39:3–8

Franck P, Nabet P, Dousset B (1998) Applications of infrared spectroscopy to medical biology. Cell Mol Biol 44:273–275

Gewert K (1999) Molecular reaction mechanisms of proteins monitored by time-resolved FTIR spectroscopy. Biol Chem 380:931–935

Gopas J, Ono M, Princler G, Smith MR, Tainsky MA, Siddiqui MAQ, Wisjniak O, Segal S, Kuwano M, Kung HF (1992) EGF receptor and mitogenic response of Balb/c 3T3 cells expressing *ras* and myc oncogenes. Cell Mol Biol 38:605–614

Jackson M, Kim K, Tetteh J, Mansfield JR, Dolenko B, Somorjai RL, William Orr F, Watson PH, Mantsch HH (1998) Cancer diagnosis by infrared spectroscopy: methodological aspects. SPIE 3257:24–34

Kumar R, Sukumar S, Barbacid M (1990) Activation of *ras* oncogenes preceding the onset of neoplasia. Science 248:1101–1104

Lacal J, Carnero A (1994) Regulation of *ras* proteins and their development in signal transduction pathways. Oncol Rep 1:677–693

Lasch P, Naumann D (1998) FT-IR microspectroscopic imaging of human carcinoma thin sections based on pattern recognition techniques. Cell Mol Biol 44:189–202

Little JB (2000) Radiation carcinogenesis. Carcinogenesis 21:397–404

Lohr M, Maisonneuve P, Lowenfels AB (2000) K-*ras* mutations and benign pancreatic disease. Int J Pancreatol 27:93–103

Lucassen GW, Caspers PJ, Pupples GJ (1998) In vivo infrared and Raman spectroscopy of human stratum corneum. SPIE 3257:52–60

Mantsch HH, Chapman D (eds) (1996) Infrared spectroscopy of biomolecules. Wiley, New York

Momchilova A, Markovska T, Pankov R (1999) Ha-*ras* transformation alters the metabolism of phophotidylethanolamine and phosphotidylcholine in NIH 3T3 fibroblasts. Cell Biol Int 23:603–610

Mordechai S, Argov S, Salman A, Cohen B, Jagannathan R, Erukhimovitch V, Goldstein J, Sinelnikov I (2000) FTIR microscopic comparative study on normal, premalignant and malignant tissues of human intestine. SPIE 4129:231–242

Parker FS (1971) Application of infrared spectroscopy in biochemistry, biology and medicine. Plenum, New York

Quincoces AF, Polanco I, Thomson T, Leon J (1997) Positive autoregulation of *ras* genes expression in fibroblasts. FEBS Lett 416:317–323

Rosenberg N, Jolicoeur P (1997) Retroviral pathogenesis. In: Coffin JM, Hughes SH, Varmus HE (eds) Retroviruses. Cold Spring Harbor Laboratory Press, Cold Spring Harbor, New York, pp 475–585

Scully C, Field JK, Tanzawa H (2000) Genetic aberrations in oral or head and neck squamous cell carcinoma 2: chromosomal aberrations. Oral Oncol 36:311–327

Tainsky MA, Shamanski FL, Blair D, Vande Woude G (1987) Human recipient cell for oncogene transfection studies. Mol Cell Biol 7:1280–1284

Tockman MS (1996) Clinical detection of lung cancer progession markers. J Cell Biochem 25:177–184

Tsai M, Yu C, Stacey D (1989) The effect of GTPase activating protein upon *ras* is inhibited by mitogenically responsive lipids. Science 243:522–526

Tsao H (2000) Update on familial cancer syndromes and the skin. J Am Acad Dermatol 42:939–969